Water vapor assisted aramid nanofiber reinforcement for strong, tough and ionically conductive organohydrogels as high-performance strain sensors

Yongchuan Wu[a, 1], Ya Zhang[a, 1], Zimin Liao[a], Jing Wen[a], Hechuan Zhang[a], Haidi Wu[a], Zhanqi Liu[a], Yongqian Shi [b], Pingan Song [c], Longcheng Tang[d], Huaiguo Xue[a], Jiefeng Gao[*a]

[a] *School of Chemistry and Chemical Engineering, Yangzhou University, No 180, Road Siwangting, Yangzhou, Jiangsu, 225002, China.*

[b] *College of Environment and Safety Engineering, Fuzhou University, Fuzhou 350116, China*

[c] *Centre for Future Materials, University of Southern Queensland, Springfield Campus, QLD 4300, Australia*

[d] *College of Material, Chemistry and Chemical Engineering, Key Laboratory of Organosilicon Chemistry and Material Technology of MoE, Key Laboratory of Silicone Materials Technology of Zhejiang Province, Hangzhou Normal University, Hangzhou 311121, China*

[1] These authors contribute equally to this article and should be considered as co-first authors.

*Corresponding author: E-mail address: jfgao@yzu.edu.cn

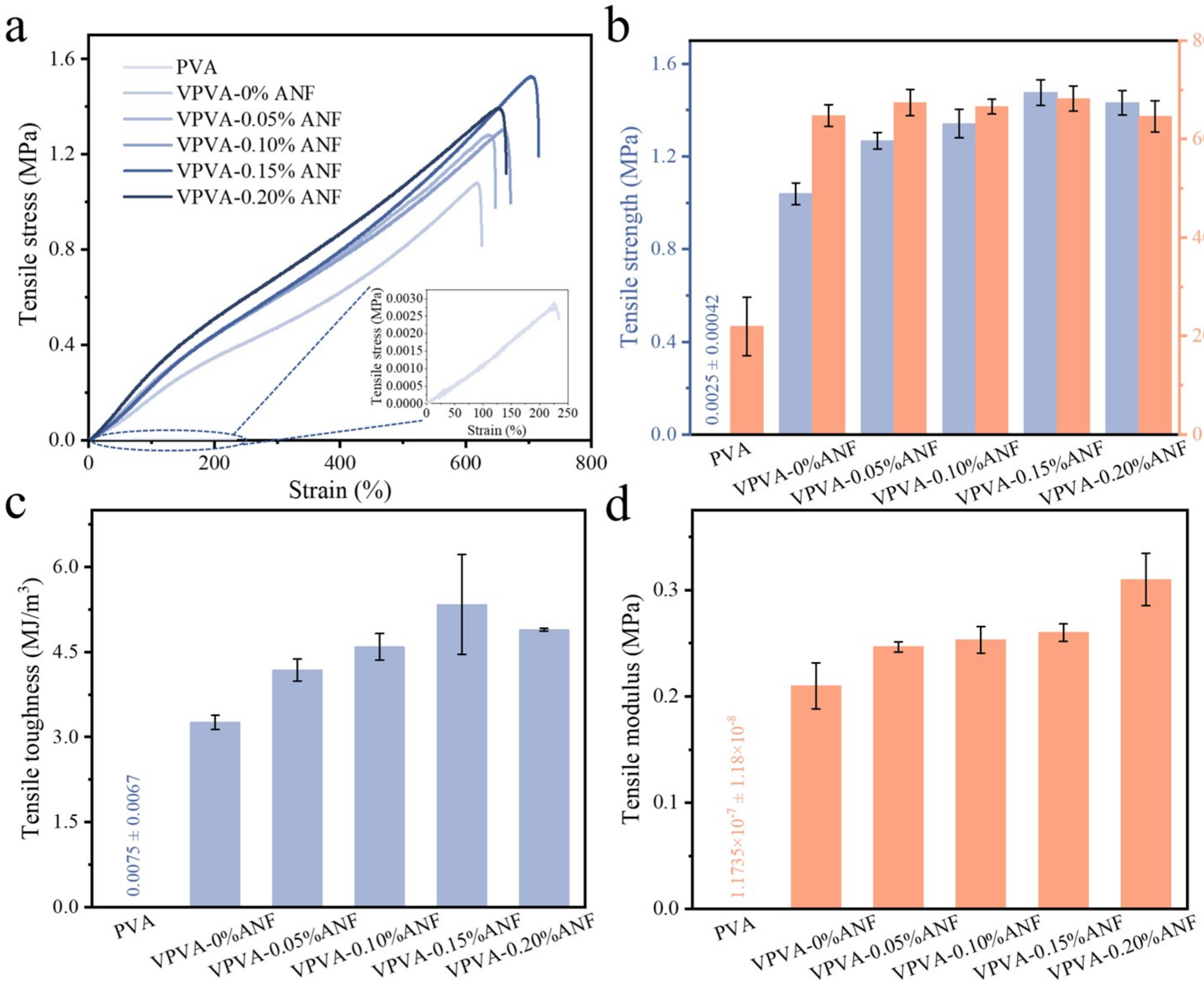

Figure S1. (a) Stress-strain curve, (b) the corresponding tensile strength and tensile strain, (c) tensile toughness and (d) tensile modulus of PVA organogel and VPVA-ANF organohydrogels with different mass fractions of ANF.

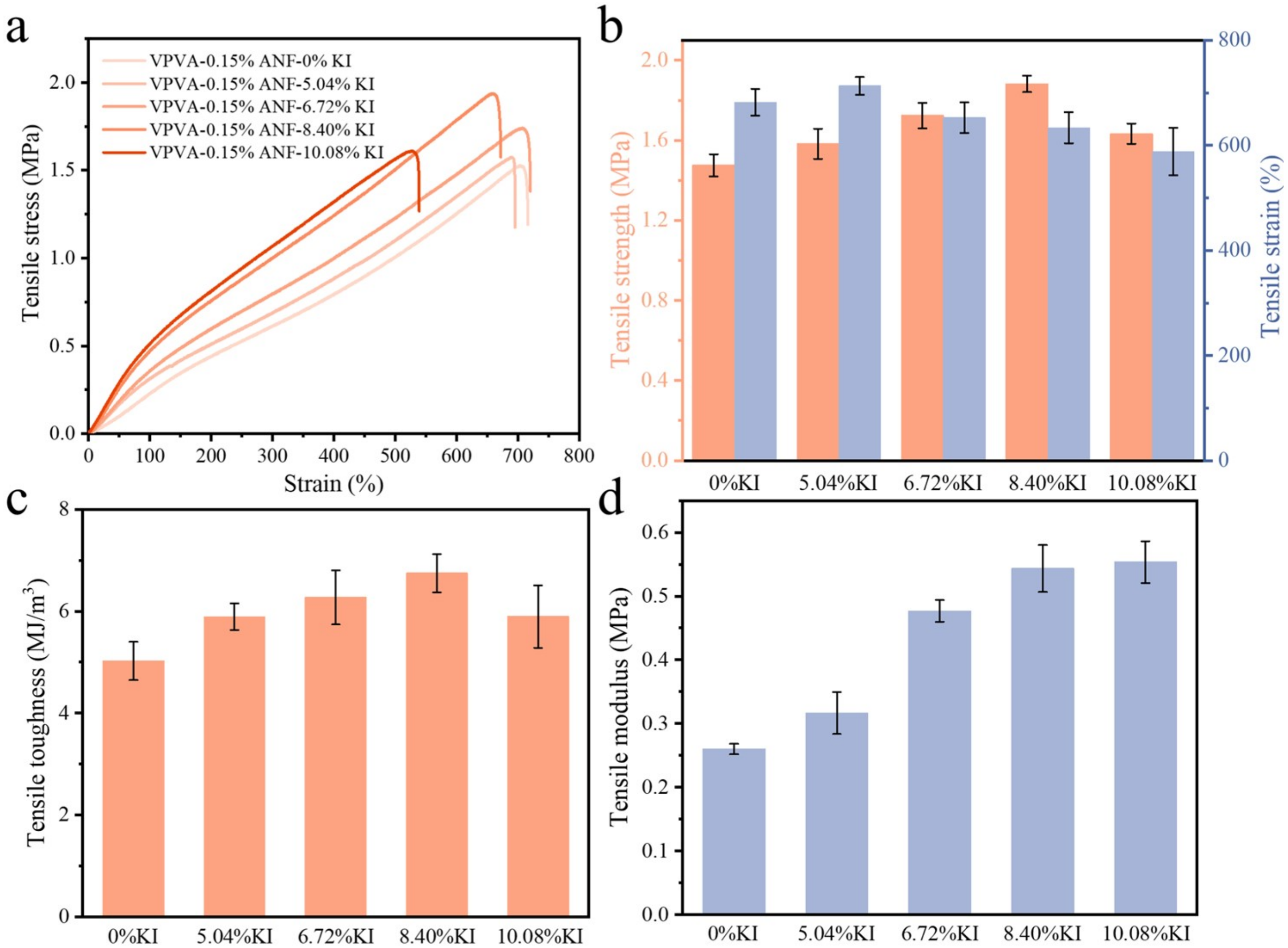

Figure S2. (a) Stress-strain curve, (b) the corresponding tensile strength and tensile strain, (c) tensile toughness and (d) tensile modulus of VPVA-ANF-KI organohydrogels with different mass fractions of KI.

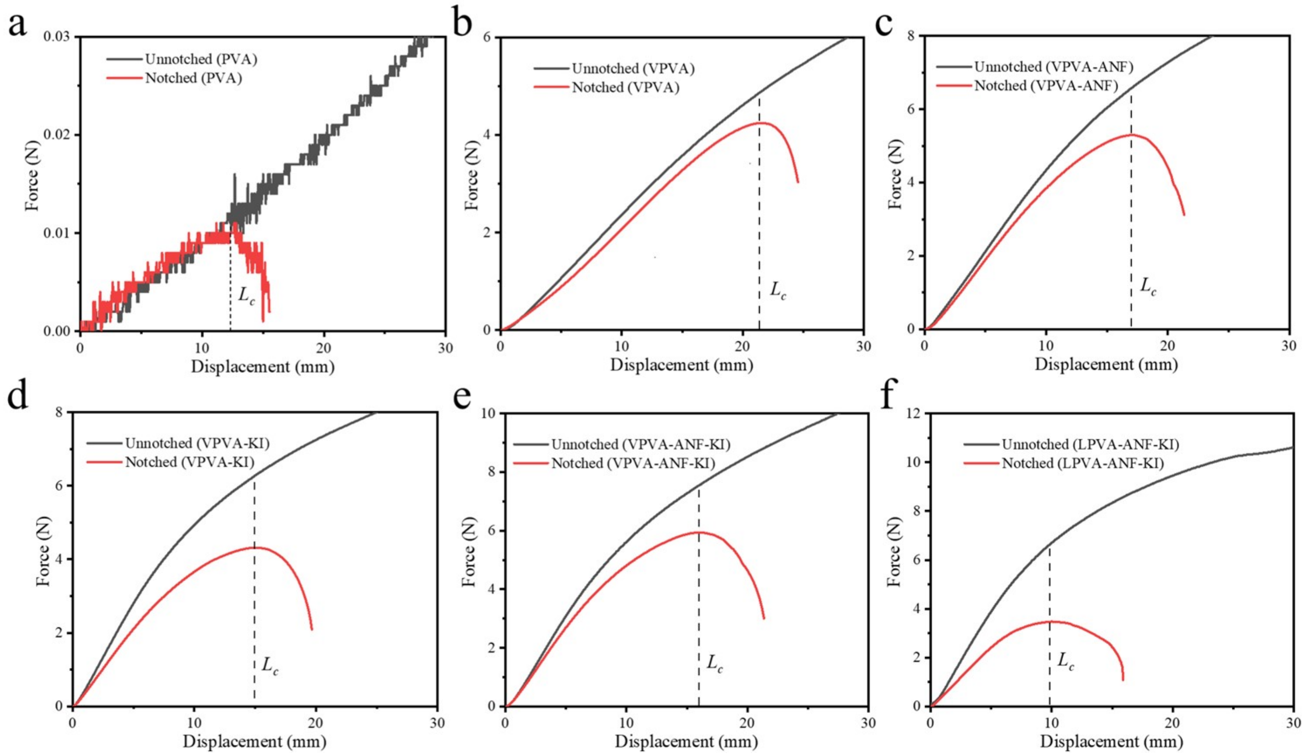

Figure S3. The force-displacement curves of unnotched and notched (a) PVA, (b) VPVA, (c) VPVA-ANF, (d) VPVA-KI, (e) VPVA-ANF-KI and (f) LPVA-ANF-KI.

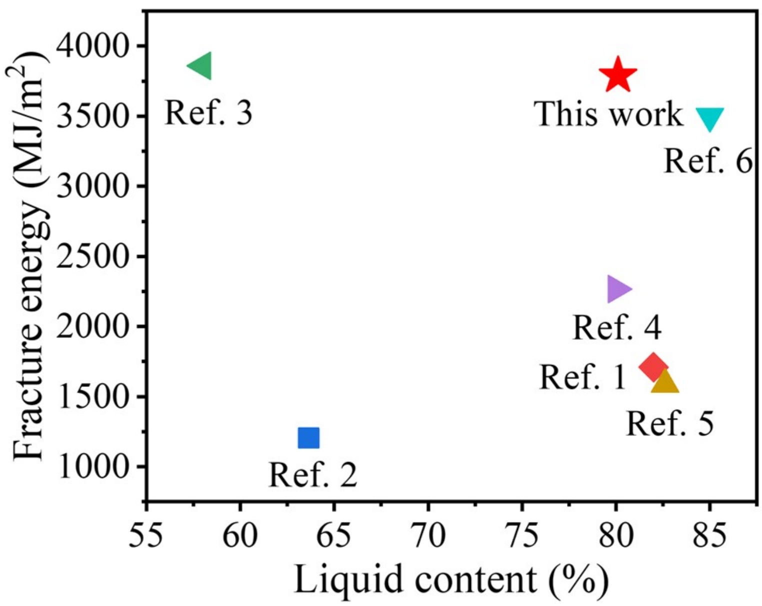

Figure S4. Comparison chart by plotting the facture energy versus liquid content among tough organohydrogels, (i.e., PVA/Gly-1,[1] PVA/P(AM-co-SBMA)/$CaCl_2$/Gly,[2] BSA/PAAm/Gly,[3] PAAm/PAA/PAD/CNT/Gly,[4] PVA/Gly-2,[5], and PVA/EG[6]).

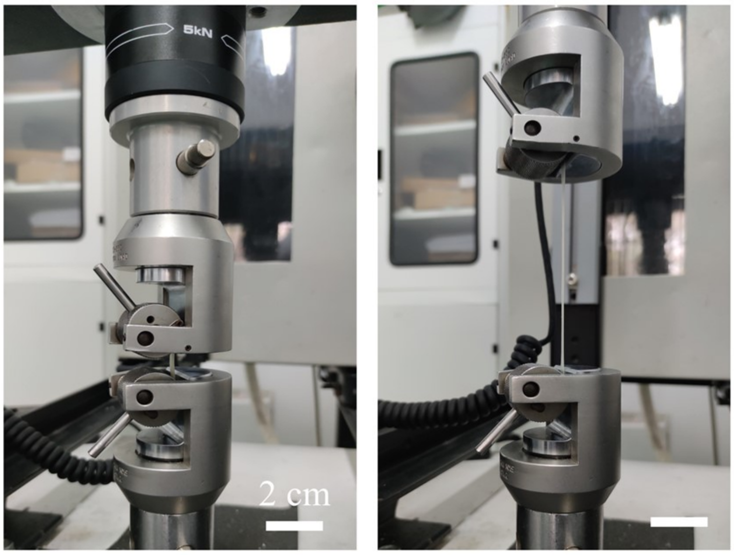

0% strain over 600% strain

Figure S5. The image showing the VPVA-ANF-KI organohydrogel with an elongation exceeding 600% of its original length.

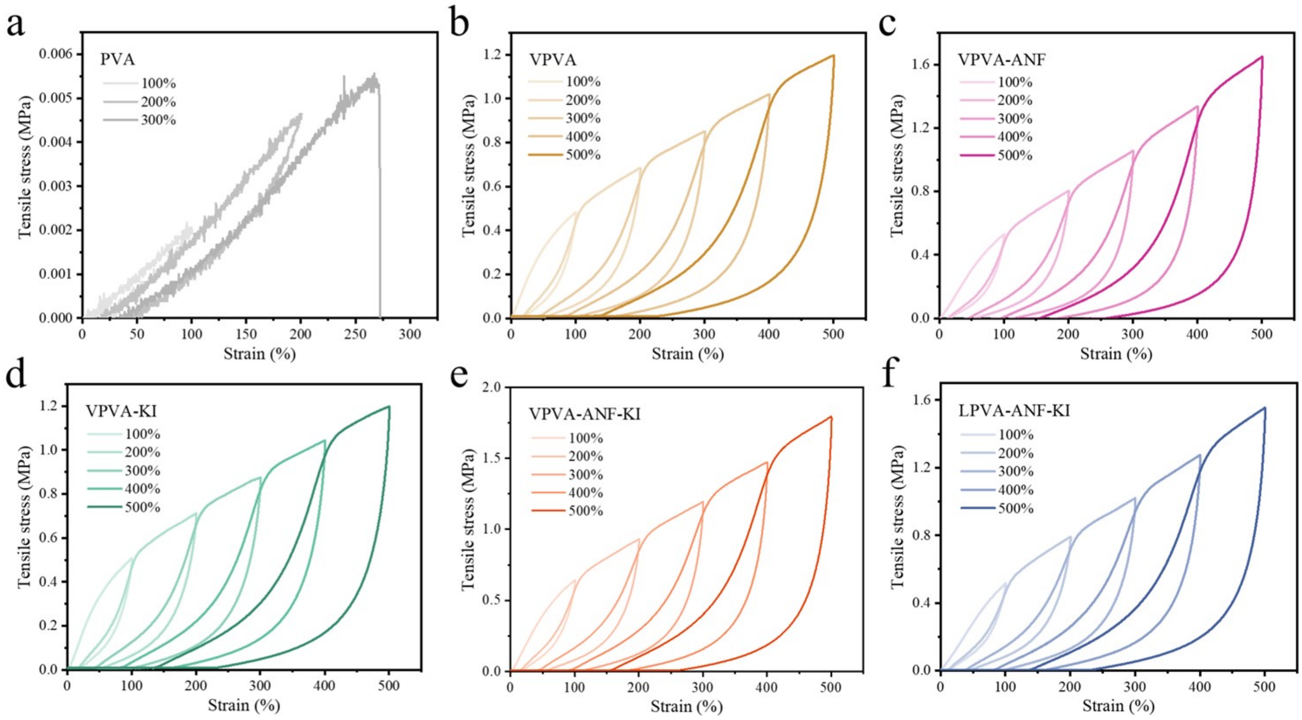

Figure S6. Sequential tensile loading-unloading tests without interval under incremental strains for (a) PVA, (b) VPVA, (c) VPVA-ANF, (d) VPVA-KI, (e) VPVA-ANF-KI and (f) LPVA-ANF-KI.

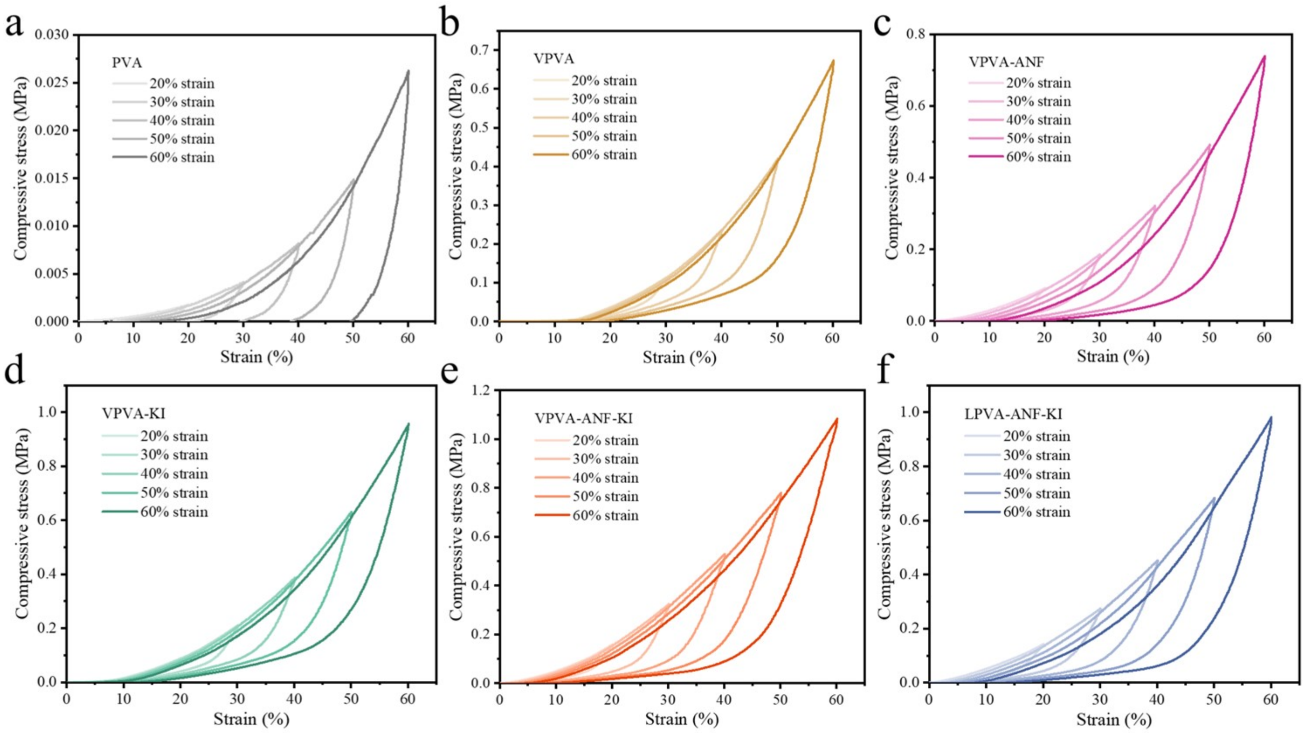

Figure S7. Sequential compressive loading-unloading tests without interval under incremental strains for (a) PVA, (b) VPVA, (c) VPVA-ANF, (d) VPVA-KI, (e) VPVA-ANF-KI and (f) LPVA-ANF-KI.

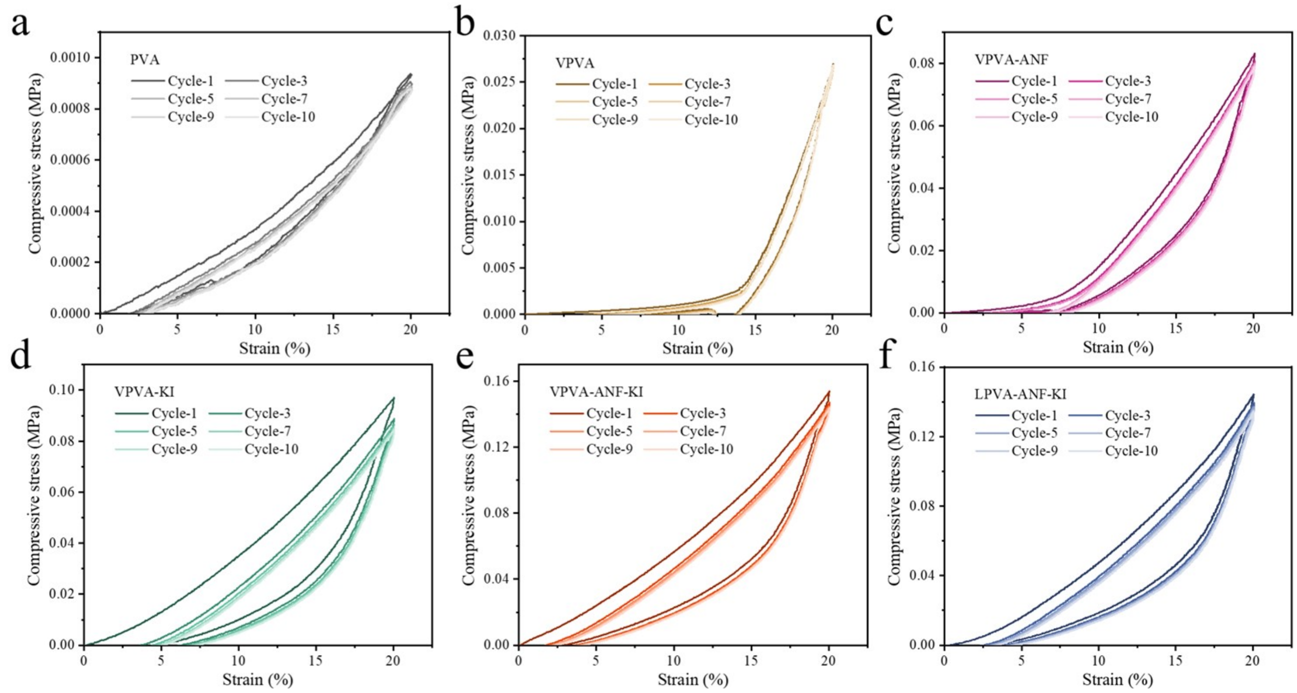

Figure S8. Cyclic stress-strain curves are shown for (a) PVA, (b) VPVA, (c) VPVA-ANF, (d) VPVA-KI, (e) VPVA-ANF-KI and (f) LPVA-ANF-KI subjected to 10 cycles of 20% compressive strains.

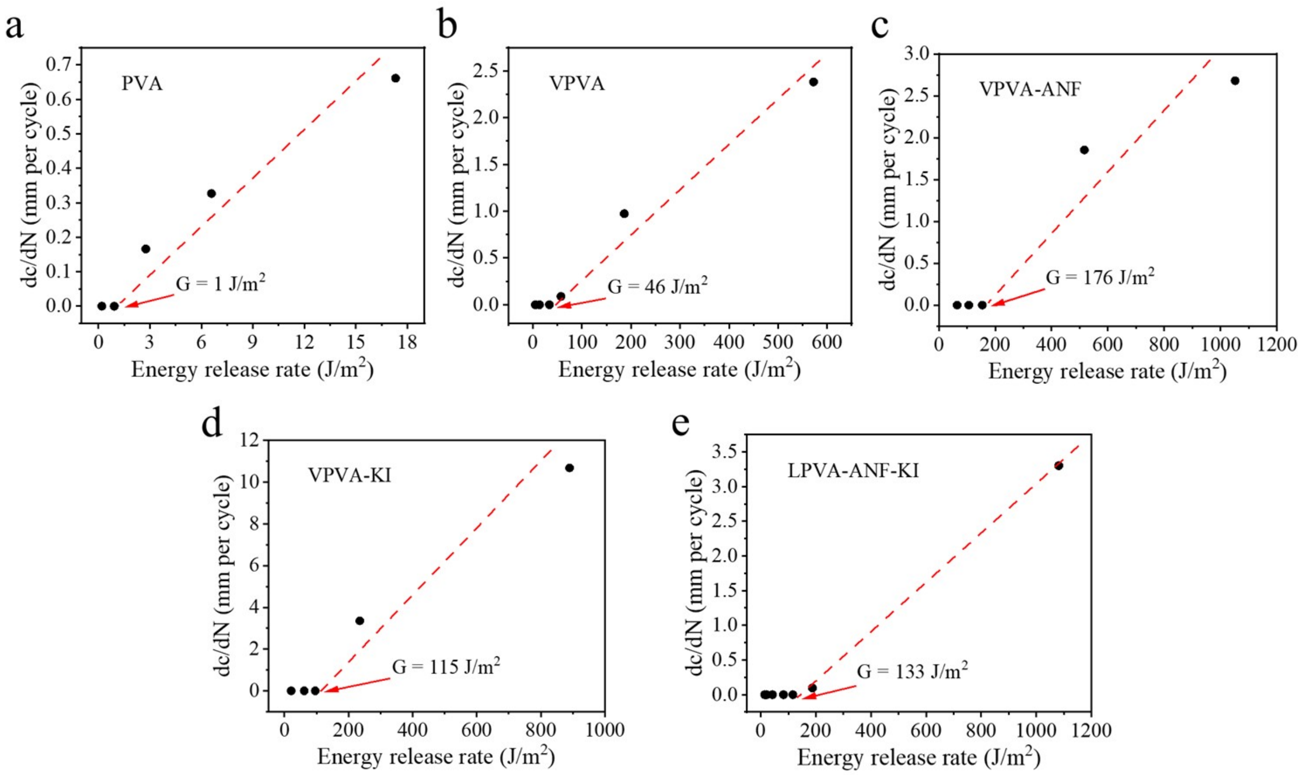

Figure S9. Crack extension per cycle dc/dN versus applied energy release rate for (a) PVA, (b) VPVA, (c) VPVA-ANF, (d) VPVA-KI and LPVA-ANF-KI.

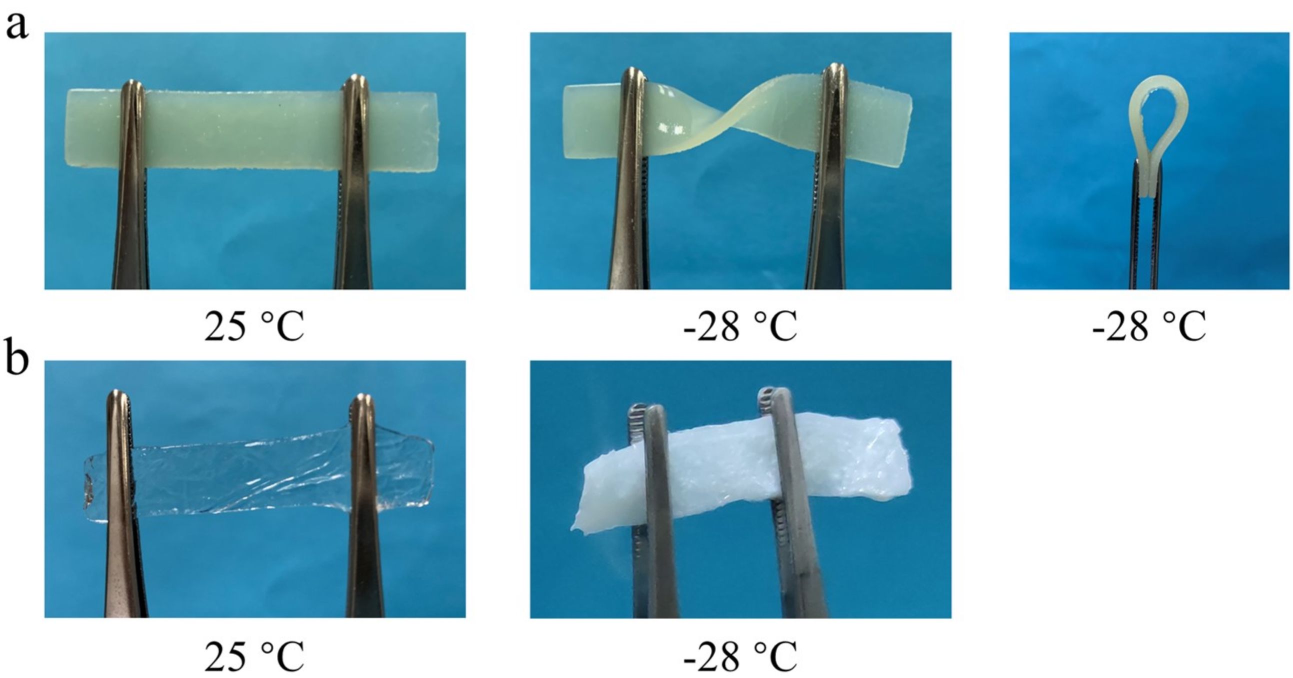

Figure S10. Photographs of the anti-freezing behavior of (a) the VPVA-ANF-KI organohydrogel and (b) PVA organogel.

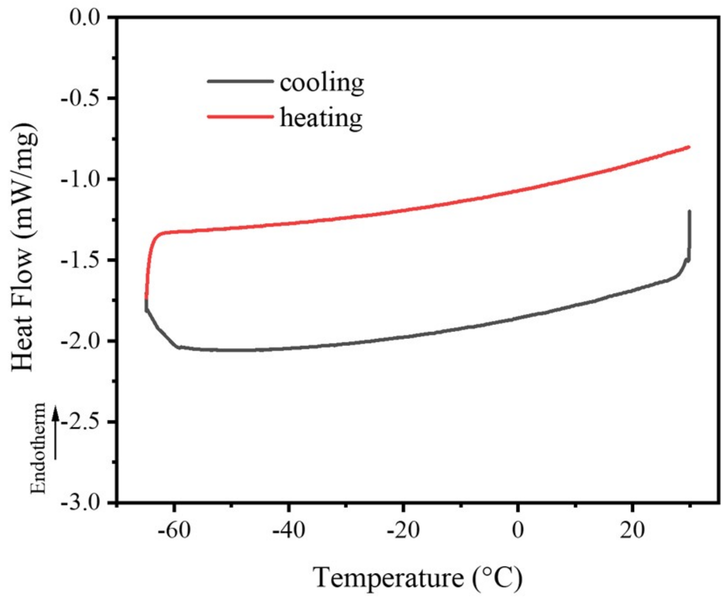

Figure S11. Heat flow curves of VPVA-ANF-KI organohydrogel during the heating and cooling process.

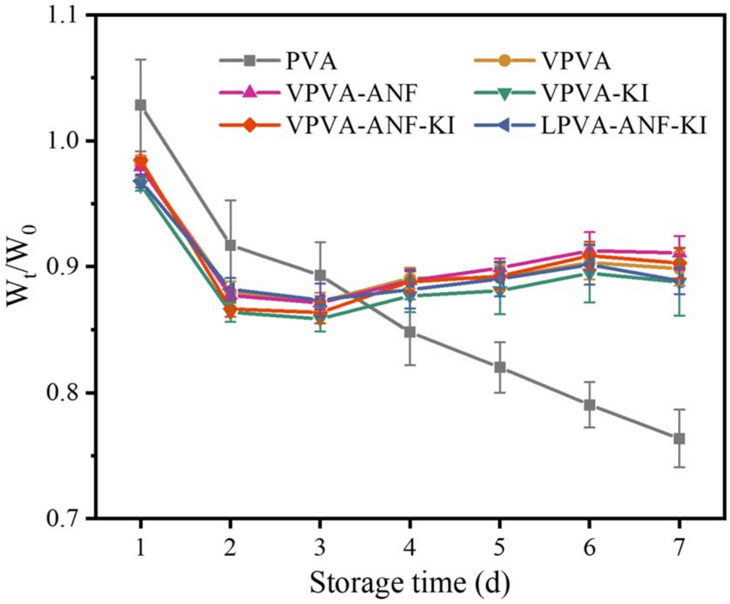

Figure S12. The weight changes of PVA, VPVA, VPVA-ANF, VPVA-KI, VPVA-ANF-KI and LPVA-ANF-KI in the normal environment for 7 d. W_0 and W_t are the initial weight and the weight in the corresponding storage days of gels.

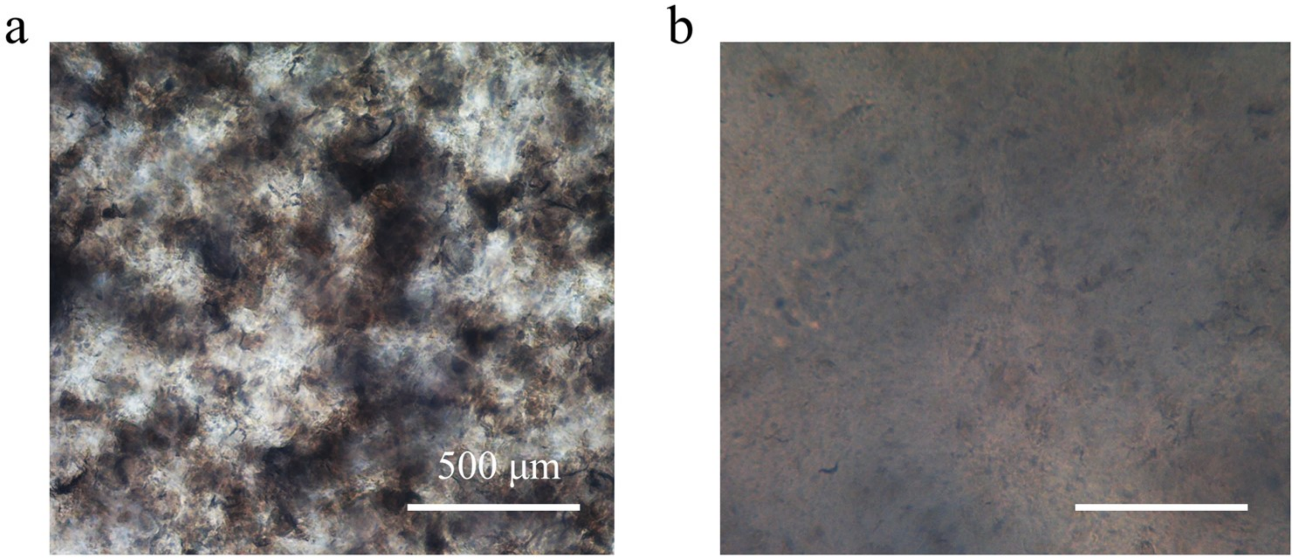

Figure S13. The optical microscope image displaying cross-section of (a) LPVA-ANF-KI and (b) VPVA-ANF-KI. Scale bar, 500 μm.

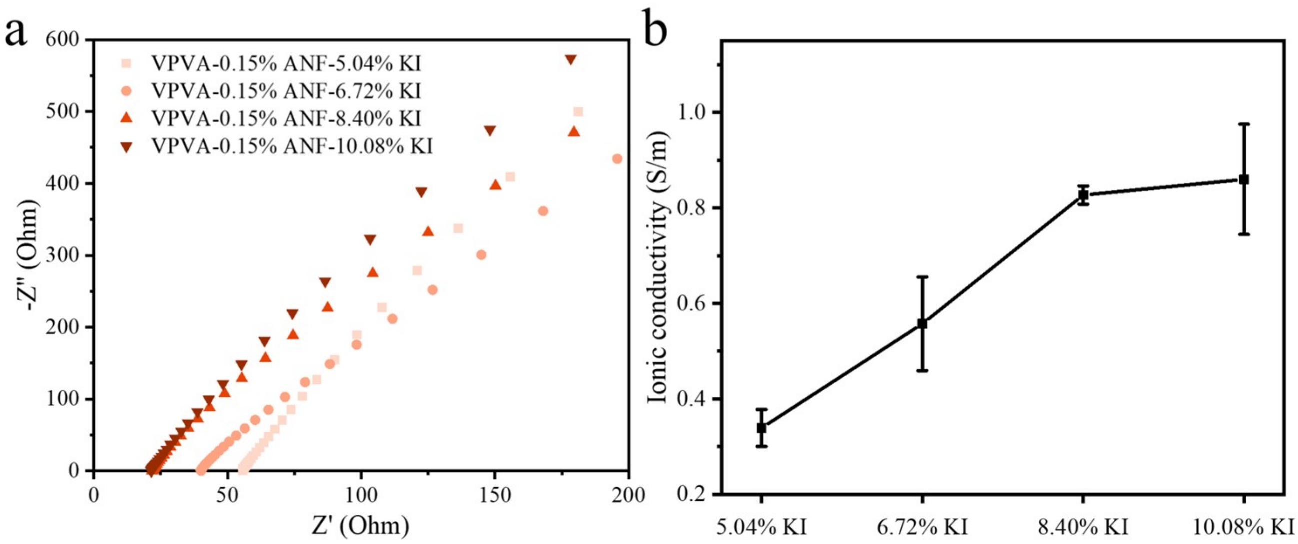

Figure S14. (a) Nyquist plots and (b) ionic conductivity of VPVA-ANF-KI with varying KI content.

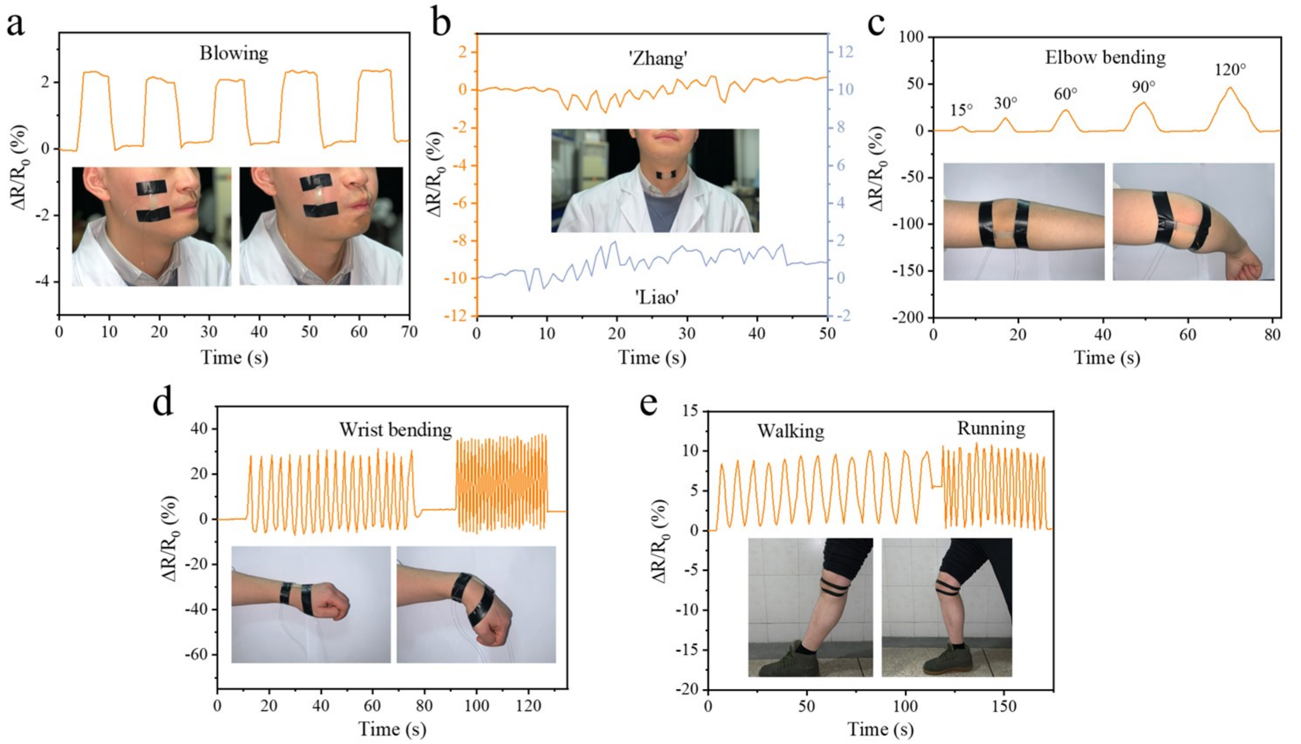

Figure S15. Demonstration of VPVA-ANF-KI sensor used for monitoring human activities, including (a) blowing, (b) voice recognizing, (c) elbow bending, (d) wrist bending and (e) walking and running.

Supplementary Table 1. A series of synthesis schemes for organogel and organohydrogels.

Sample	PVA (g)	DMSO (g)	2wt% ANF (g)	KI/DMSO (g)		Water vapor (g)	Liquid water (g)
PVA	2.25	17.59	0	0	Take 8.2g →	0	0
VPVA-0%ANF	2.25	12.75	0	0	Take 6.2g →	2	0
VPVA-0.05%ANF	2.25	12.25	0.5	0	Take 6.2g →	2	0
VPVA-0.10%ANF	2.25	11.75	1	0	Take 6.2g →	2	0
VPVA-0.15%ANF	2.25	11.25	1.5	0	Take 6.2g →	2	0
VPVA-0.20%ANF	2.25	10.75	2	0	Take 6.2g →	2	0
VPVA-0.15%ANF-5.04%KI	2.25	7.5	1.5	3.75	Take 6.2g →	2	0
VPVA-0.15%ANF-6.72%KI	2.25	6.25	1.5	5	Take 6.2g →	2	0
VPVA-0.15%ANF-8.40%KI	2.25	5	1.5	6.25	Take 6.2g →	2	0
VPVA-0.15%ANF-10.08%KI	2.25	3.75	1.5	7.5	Take 6.2g →	2	0
VPVA-8.40%KI	2.25	6.5	0	6.25	Take 6.2g →	2	0
LPVA-0.15%ANF-8.40%KI	2.25	5	1.5	6.25	Take 6.2g →	0	2

Reference

[1] S. Shi, X. Peng, T. Liu, Y.-N. Chen, C. He, H. Wang, *Polymer* **2017**, *111*, 168.
[2] O. Hu, J. Lu, S. Weng, L. Hou, X. Zhang, X. Jiang, *Polymer* **2022**, *254*, 125109.
[3] J. Yang, Z. Liu, K. Li, J. Hao, Y. Guo, M. Guo, Z. Li, S. Liu, H. Yin, X. Shi, G. Qin, G. Sun, L. Zhu, Q. Chen, *ACS Appl. Mater. Interfaces* **2022**, *14*, 39299.
[4] L. Han, K. Liu, M. Wang, K. Wang, L. Fang, H. Chen, J. Zhou, X. Lu, *Adv. Funct. Mater.* **2018**, *28*, 1704195.
[5] Y. Wu, W. Xing, J. Wen, Z. Wu, Y. Zhang, H. Zhang, H. Wu, H. Yao, H. Xue, J. Gao, *Polymer* **2023**, *267*, 125661.
[6] J. Yang, J. Hao, C. Tang, Y. Guo, M. Guo, Z. Li, S. Liu, H. Yu, G. Qin, Q. Chen, *Journal of industrial and engineering chemistry* **2022**, *116*, 207.